Study of Ionospheric Conductivity Dependence of Subauroral Polarization Streams Observed by the SuperDARN HF Radar Network

SuperDARN短波レーダーネットワークによるサブオーロラ帯高速流の電気伝導度依存性の研究

Y. Zhang, N. Nishitani, and T. Hori (ISEE, Nagoya University)

Contents

Introduction-*What is SAPS?*

SAPS (SubAuroral Polarization Stream) is caused by strong electric fields oriented poleward in the ionosphere, and is defined as relatively narrow channel of enhanced westward flow, located equatorward of the auroral oval.

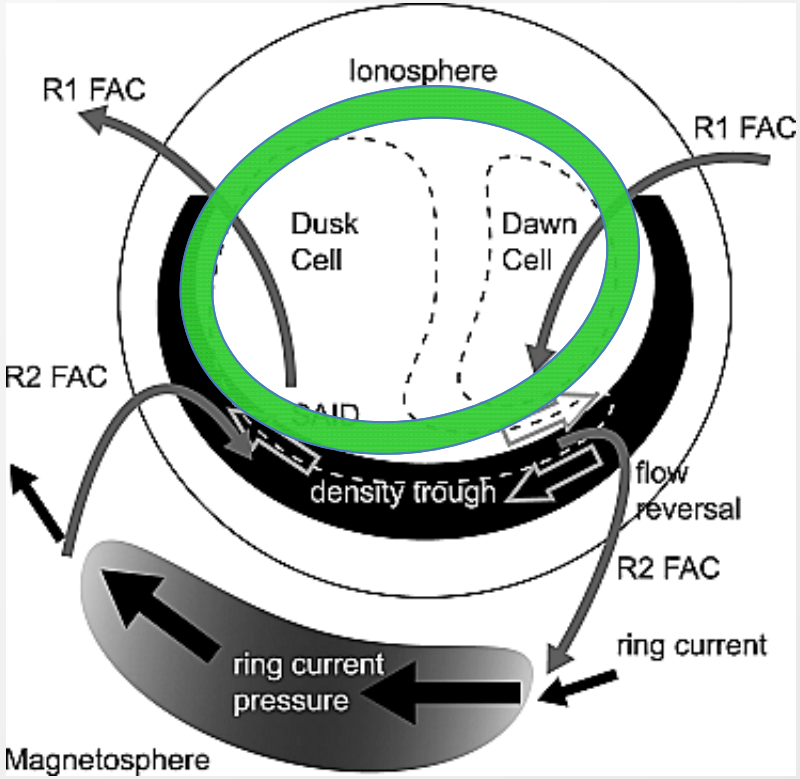

Fig 1. The generation of SAPS [Kataoka et al., 2007].

- SAPS occurs at lower latitude as the MLT(Magnetic Local Time) progresses [Foster and Vo, 2002].
- The latitude of SAPS is related to Dst value [Kataoka et al, 2009]

Motivation & Purpose

- Previous studies have reported the characteristics and morphologies of SAPS.
- In contrast, the change in SAPS in response to solar illumination has so far not been fully investigated.
- To understand the mechanism and the characteristics of SAPS in more details, it is necessary to investigate the influence of solar illumination upon SAPS.

Using SuperDARN Hokkaido and Buckland Park HF Radar to study the influence of solar illumination upon SAPS

Instrumentations

- SuperDARN Hokkaido East Radar
  Location: +36.76, -144.78
  (AACGM magnetic coordinates)

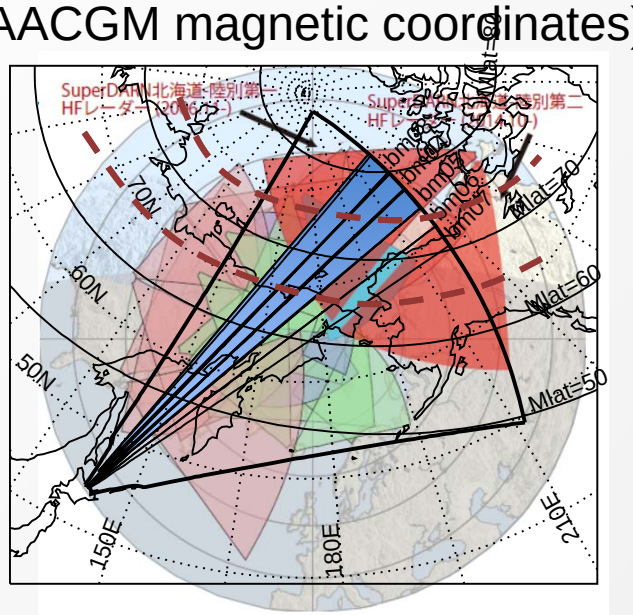

Fig 2. Radar map of the northern hemisphere [Nishitani,2014].

- SuperDARN Buckland Park Radar
  Location: -46.2, -146.1
  (AACGM magnetic coordinates)

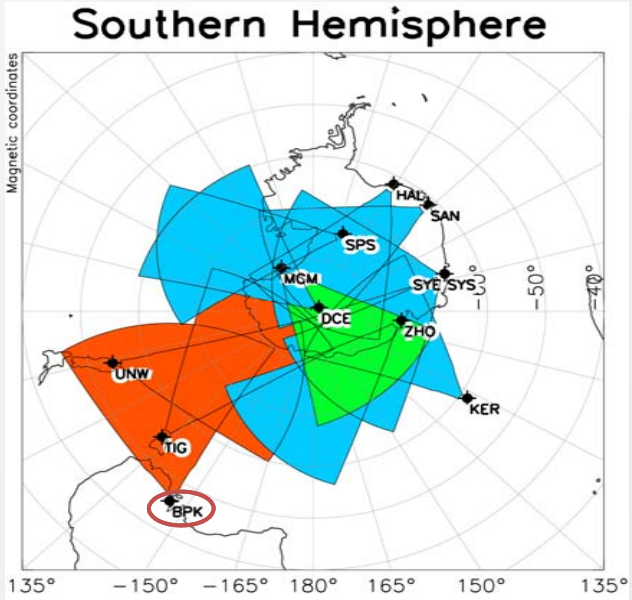

Fig 3. Radar map of the western hemisphere [http://vt.superdarn.org/tiki-index.php?page=Radar+Overview].

- NOAA POES (Polar-orbiting Operational Environmental Satellites) Satellite System

The POES satellite system makes nearly polar orbits 14 times per day. We can examine the precipitating energy flux obtained from the total electron detector (TED) onboard the NOAA POES satellites.

Analysis

- Date: 2008/01/10 to 2016/12/31

  Total over 3180 days

- Time period: 0300 ~ 0800 UT (12 ~ 17 LT)

- Conditions to define SAPS:
  - LOS (Line of Sight) Velocity > 150 m/s.
  - Duration longer than 5 min.
  - Locate at subauroal region (equatorward of auroral oval).

Analysis

- The region where precipitation flux is over $1\ mW/m^2$ is identified as auroral oval, whereas that equatorward of the oval where the flux is below the above value is identified as subauroral region [Yahnin et al., 1997].

– Cyan color :

flux $> 1\ mW/m^2$

– Blue color :

$0.1 <$ flux $< 1\ (mW/m^2)$

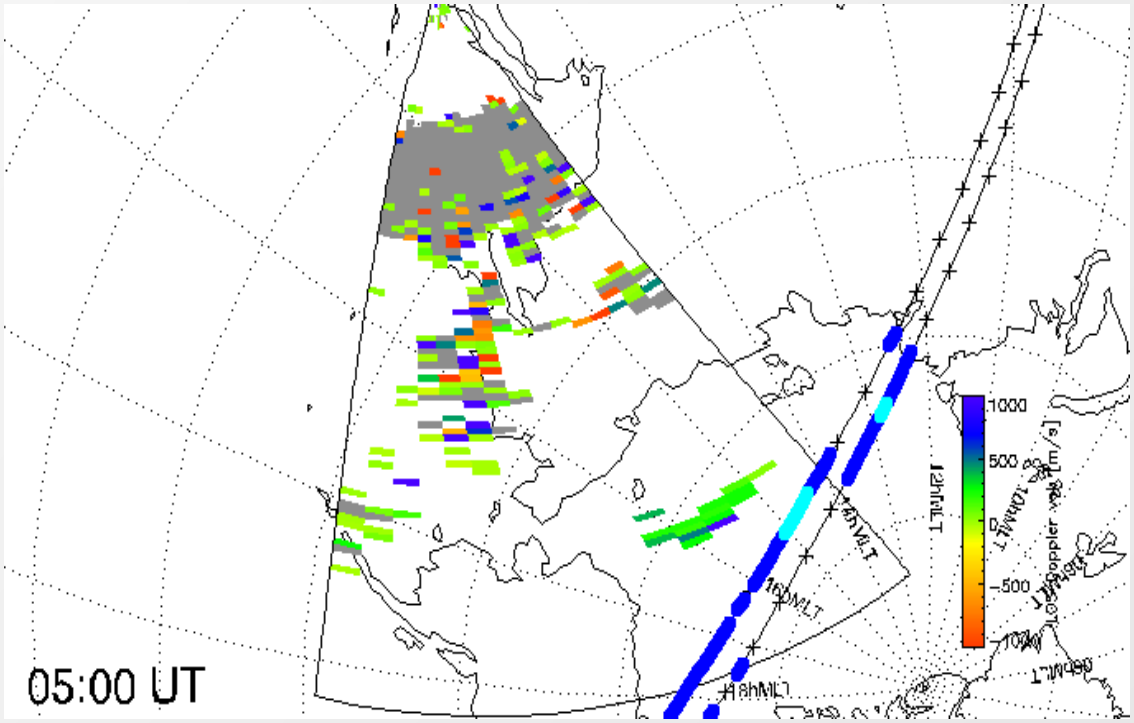

Fig 4. An sxample of SuperDARN and NOAA particle data on January 18, 2008

Analysis

Among over 3180 days, there are 60 events of Hokkaido East Radar and 5 events of Buckland Park Radar that were identified to be the SAPS.

When investigating the relation between SAPS and solar zenith angle (SZA),we chose the start, middle and end points in time of each event.

$$60 \times 3 = 180 \text{ data points}$$
$$5 \times 3 = 15 \text{ data points}$$

Result - Hokkaido East Radar

1. The relation between the SAPS velocity and SZA.

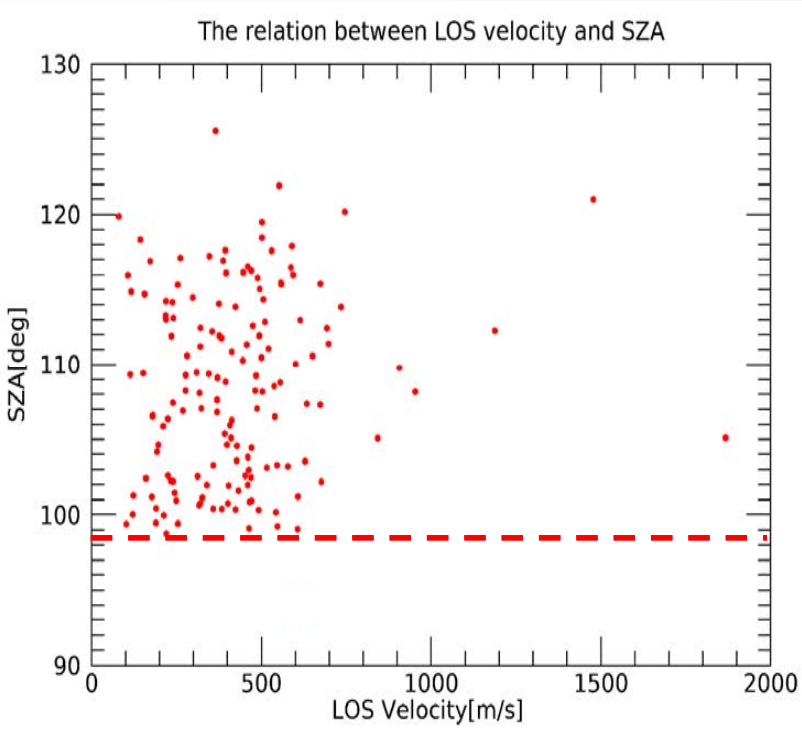

Fig 5. The relation between the SAPS velocity and SZA.

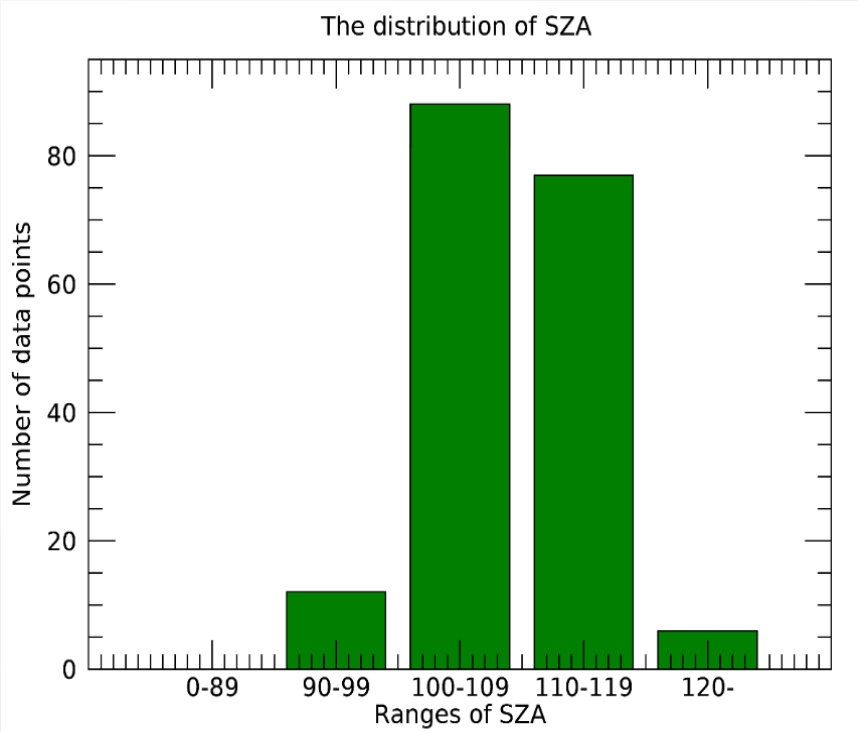

Fig 6. The distribution of the SZA of the SAPS peak LOS velocity.

- There is no clear relation between the SAPS speed and SZA.
- SAPS seems to appear more often when the SZA is larger than 98.5 degrees.

Result - Hokkaido East Radar

$$\alpha = SZA - 90°$$

$$h = \frac{R}{\cos\alpha} - R$$

$$SZA' = 98.5°, \mathrm{R} = 6378\ \mathrm{km}$$

$$\therefore h \approx 70.8\ \mathrm{km}$$

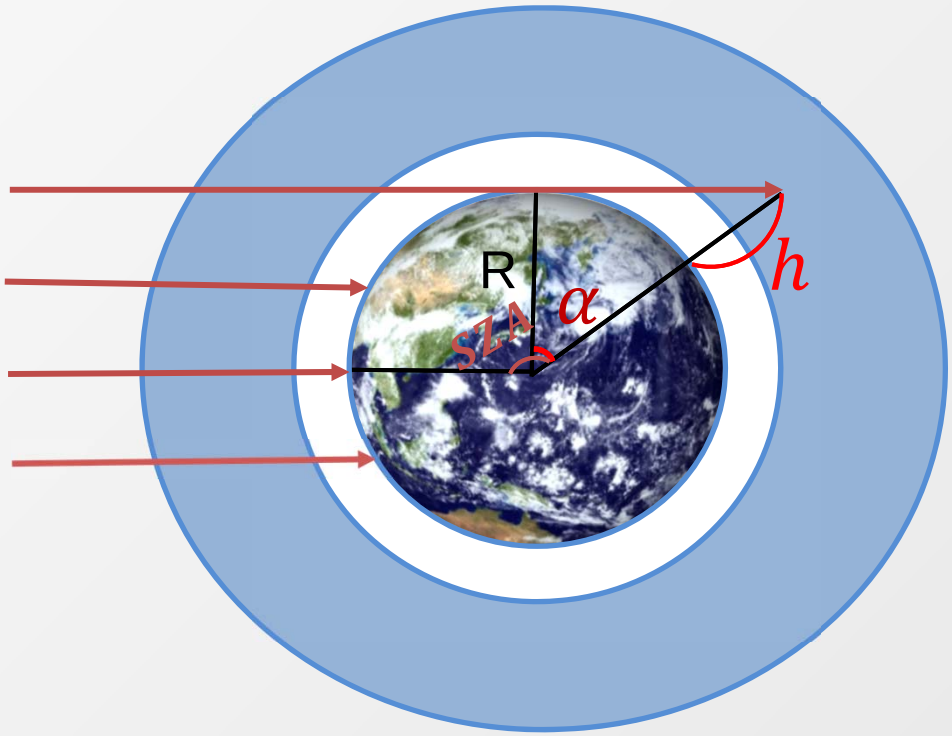

Fig 7. The simulation of solar illumination upon the earth.

When $SZA' = 98.5°$, the threshold of illuminated atmospheric altitude is 71 km.

Discussion 1

- The solar EUV passing through the atmosphere under ~ 75 km is absorbed.

- When calculating the minimal threshold of illuminated atmospheric altitude , it is necessary to add the height of the UV-absorbing atmosphere above the current result.

$$h = [\mathrm{R} + 75]/\cos(\alpha) - R \approx 146km$$

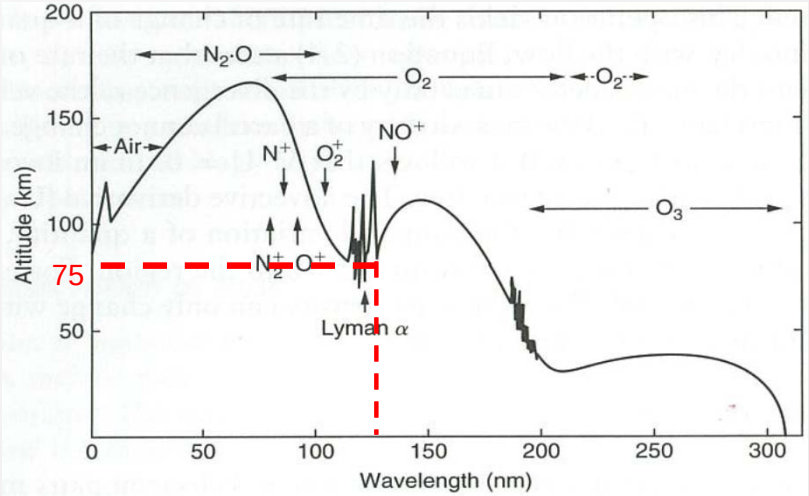

Fig 8. Depth of penetration of solar radiation as a function of wavelength.

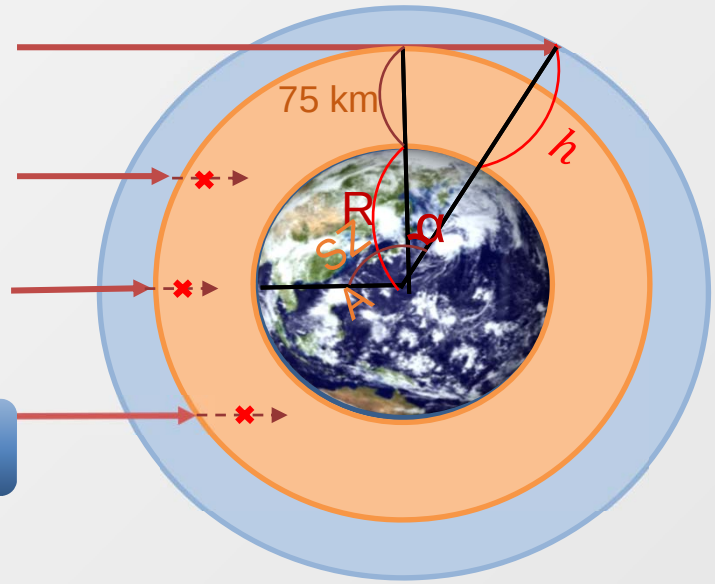

Fig 9. The simulation of solar radiation passing through the atmosphere.

Discussion 1

- The true location of the backscatter should locate towards the radar by 1~2° in geographic coordinate [Yeoman et al., 2008], which leads to 0.4 degrees of decrease in SZA, and about 8 km of decrease in illuminated ionospheric altitude h.

$$h = 138\ km$$

- h is near the altitude of the peak of Pedersen conductivity.

Pedersen conductivity plays an important role for the generation of SAPS.

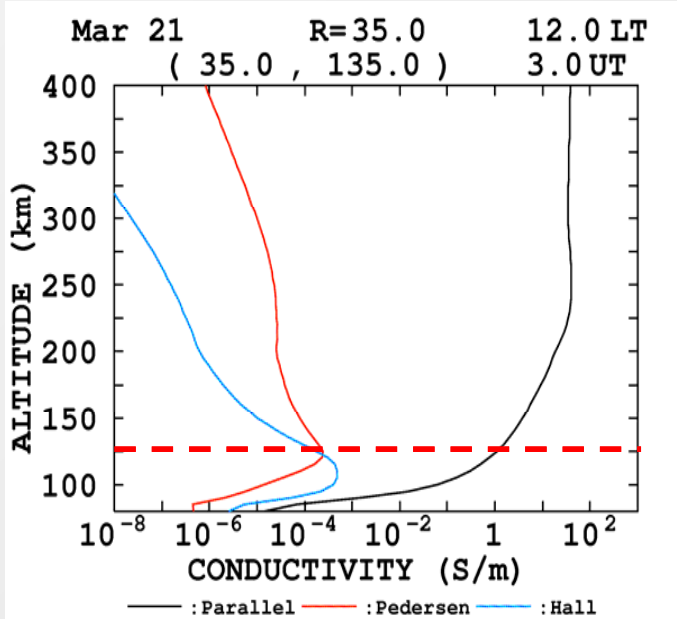

Fig 10. http://wdc.kugi.kyoto-u.ac.jp/ionocond/exp/icexp-j.html

Discussion 2

- No clear relation between SAPS speed and SZA.

① The number of the events is relatively insufficient.

② The illumination status in southern hemisphere is not considered, the impact of the southern hemisphere solar illumination on SAPS should also be considered.

- The threshold for SAPS speed is $100 \sim 200\ \mathrm{m/s}$ [Nagano et al., 2015].

$$V = \frac{v_{los}}{\cos\theta} \qquad \theta \approx 60^\circ$$

$$V > 300\ m/s$$

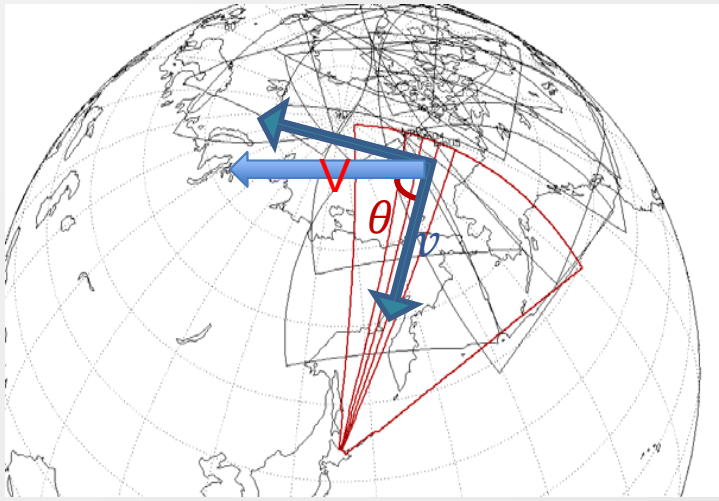

Fig 11. Light blue arrows represent SAPS speed, while the dark blue arrow along the beam represent LOS velocity.

Discussion 3 (Chisham et al., 2008)

- The standard virtual height model:
  - Assume a straight line virtual propagation path.
  - Assume that the real and virtual propagation paths have approximately the same ground range.
  - Single virtual height value (h_i) is assumed for most F-region backscatter, and a ½-hop backscatter is always assumed.

$$h_v = \begin{cases} \frac{115r}{150} & \text{for } 0 < r < 150\,\text{km} \\ 115 & \text{for } 150 \le r \le 600\,\text{km} \\ \frac{r-600}{200}(h_i - 115) + 115 & \text{for } 600 < r < 800\,\text{km} \\ h_i & \text{for } r \ge 800\,\text{km} \end{cases}$$

Fig 12. The standard model used for SuperDARN backscatter [Chisham et al., 2008].

Typical ground errors were larger than 16 km for ½-hop F-region backscatter and 60 km for 1½-hop F-region backscatter.

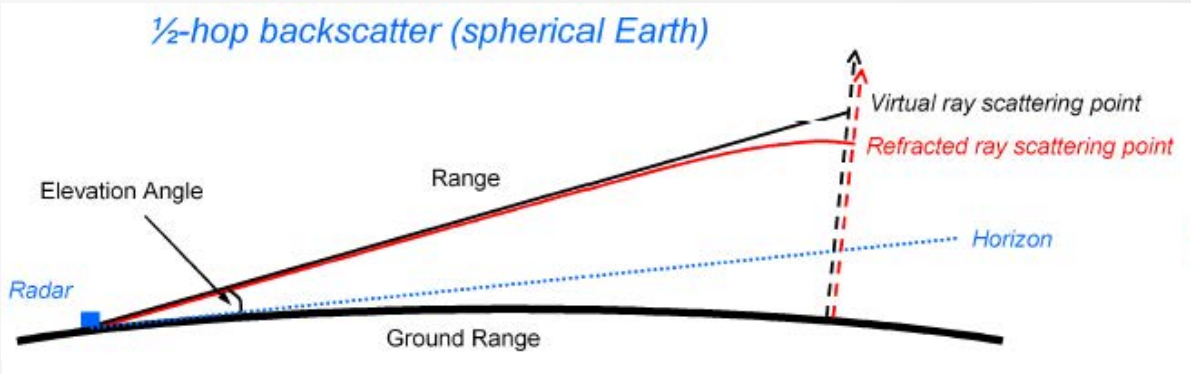

Fig 13. Schematic diagram illustrating refracted and virtual HF propagation paths for 1½-hop ionospheric backscatter assuming a spherical earth [Chisham et al., 2008].

Discussion 3 (Chisham et al., 2008)

- The new empirical virtual height model:
  - Based on peak virtual height.
  - Reduces the systematic uncertainties in the mapping of the locations of scattering regions, especially at far ranges.

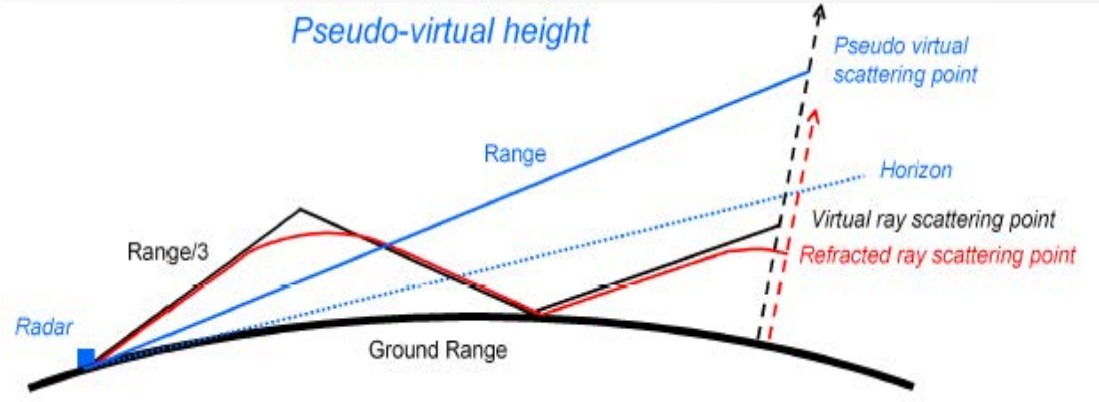

Fig 14. A simple schematic diagram illustrating the concept of pseudo virtual height for 1½ -hop backscatter

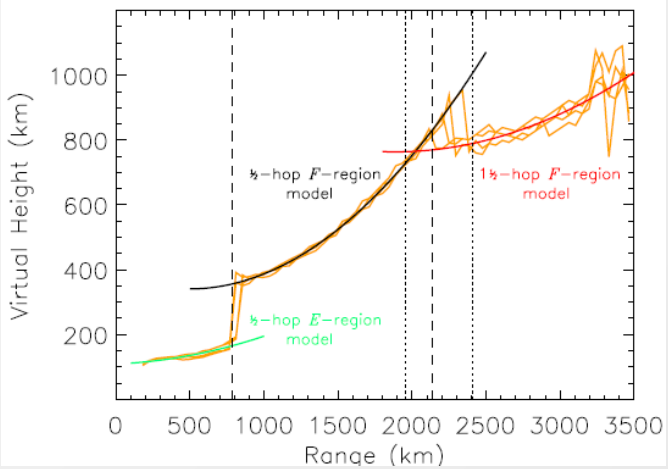

Fig 15. The virtual height models determined from the Saskatoon data set [Chisham et al., 2008].

$$h^*(r) = A + Br + Cr^2$$

Backscatter Type	A	B	C
$\frac{1}{2}$-hop E-region	108.974	0.0191271	6.68283×10^{-5}
$\frac{1}{2}$-hop F-region	384.416	−0.178640	1.81405×10^{-4}
$1\frac{1}{2}$-hop F-region	1098.28	−0.354557	9.39961×10^{-5}

Fig 16. The coefficients for the three different virtual height models [Chisham et al., 2008].

Discussion 3 (Chisham et al., 2008)

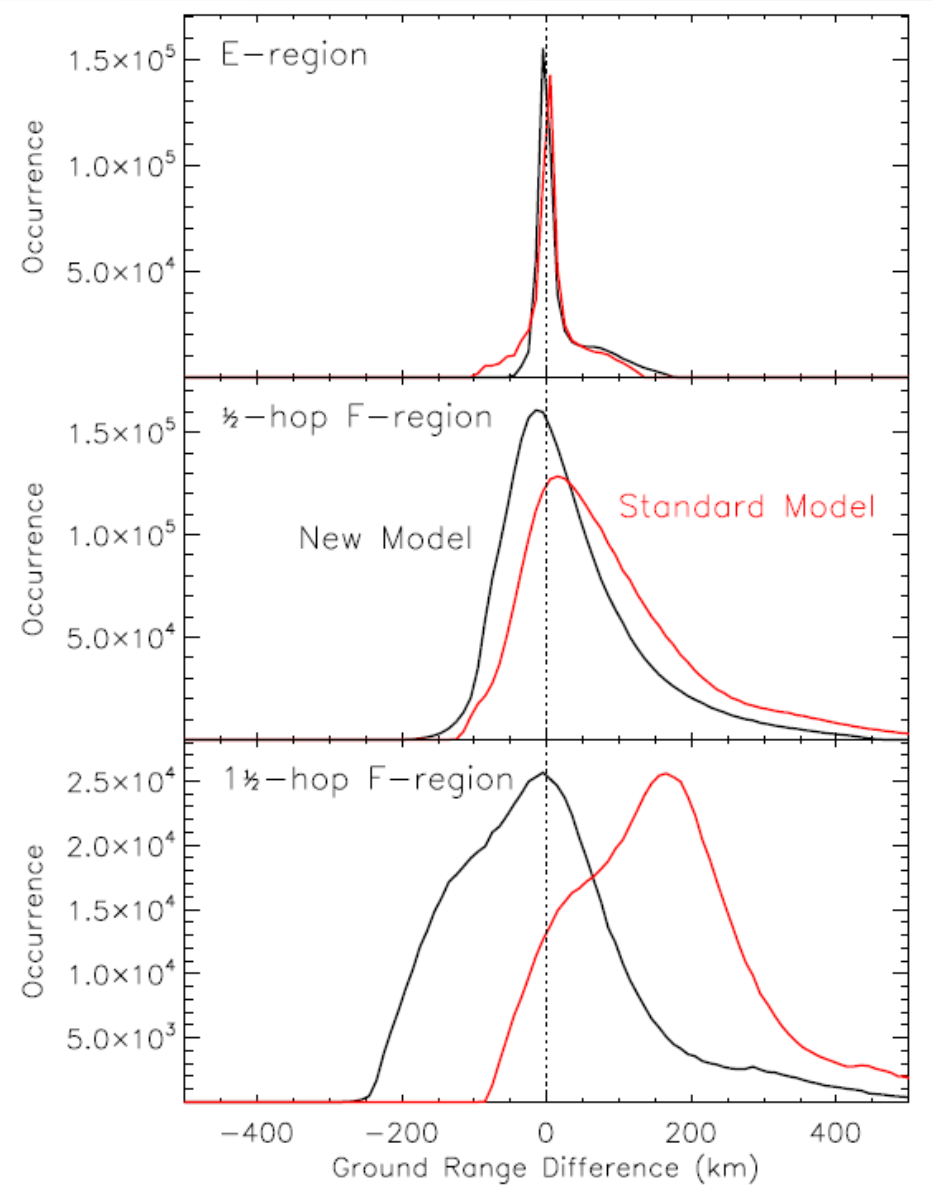

The new empirical virtual height model preform extremely well comparing to the standard virtual height model.

Fig 17. Ground range difference distributions comparing the performance of the new empirical model (black distributions) and the standard SuperDARN model (red distributions) [Chisham et al., 2008].

Result - Buckland Park Radar

1. The relation between the SAPS velocity and SZA.

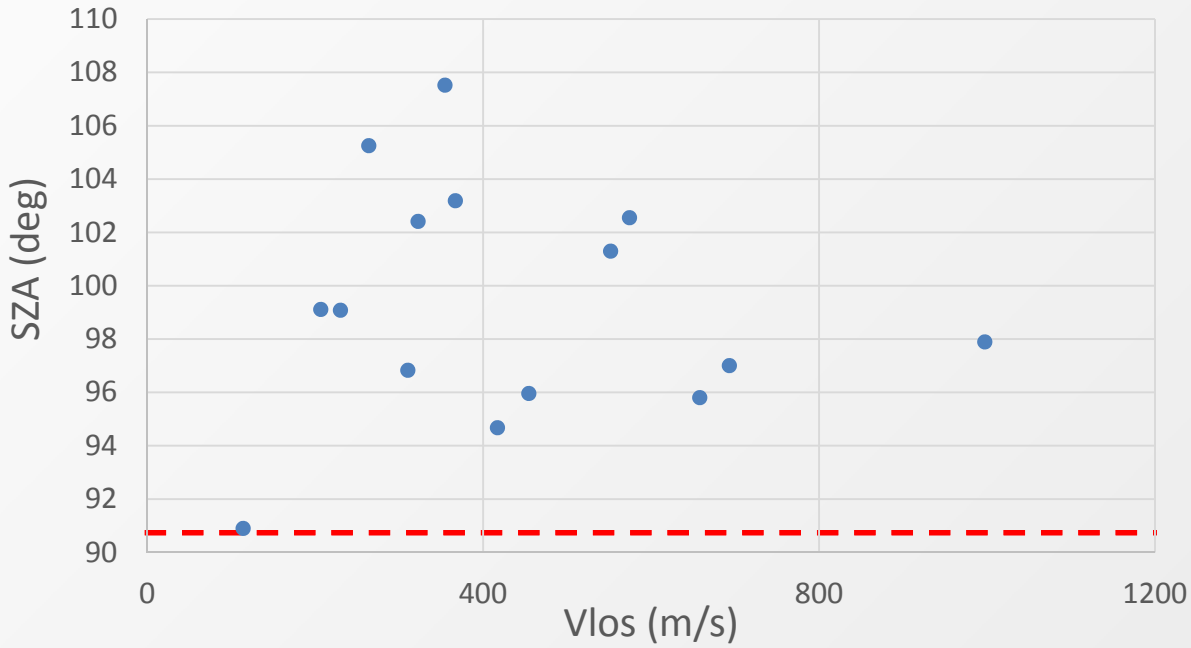

Fig 18. The relation between the SAPS velocity and SZA.

- There is no clear relation between the SAPS speed and SZA.
- SAPS seems to appear more often when the SZA is larger than about 91 degrees.

Conclusion

We checked over 3180 days from 2008/1/10 to 2016/12/31 and found 65 SAPS events during 0300 ~ 0900 UT. By investigating the relation between solar zenith angle and SAPS, the following results have been found.

- There is no clear relation between the SAPS speed and SZA.
- SAPS tends to appear when the SZA is larger than 98.5 degrees, and the threshold of illuminated atmospheric altitude is 138km for SAPS to appear. This result suggests that the Pedersen conductivity plays an important role for the generation of SAPS, which is consistent with the previous studies[Wang et al., 2008].

Future Work

- Adjust conditions to get more SAPS event.
- Check other radars' data and satellites' data.
- Apply the Chisham model to the present analysis.
- Further analysis of the data of Buckland Park Radar.

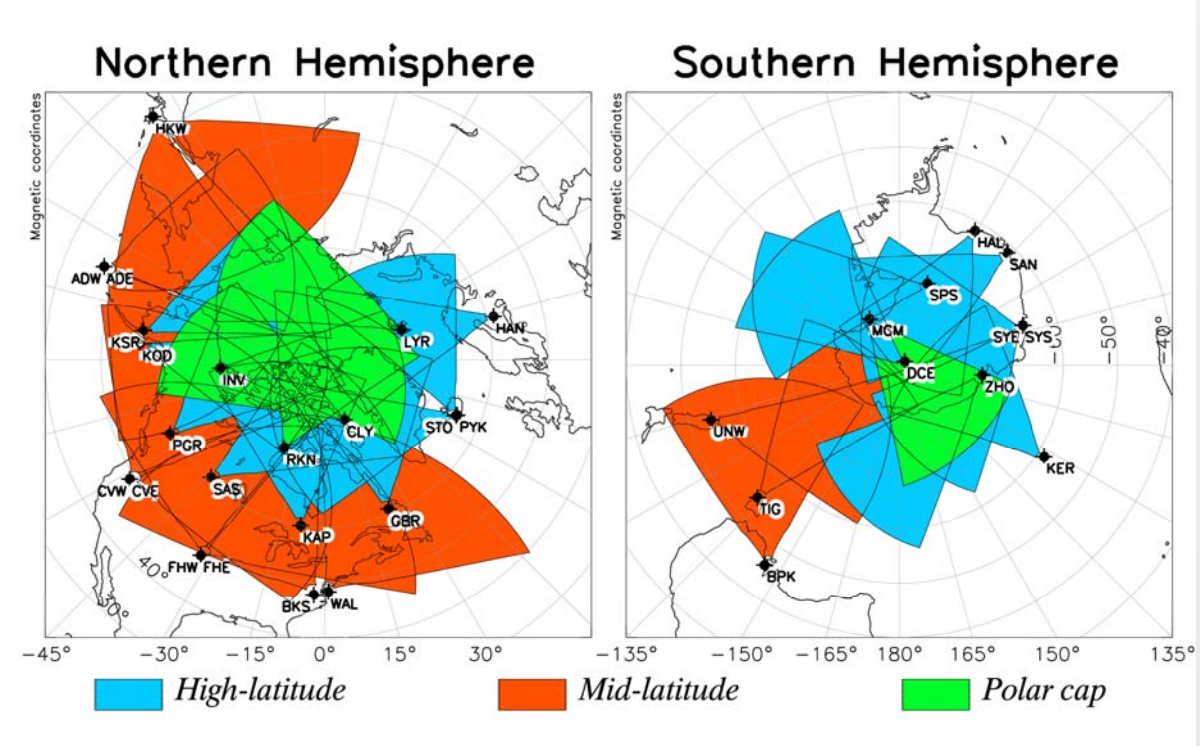

Fig 19. The map of the SuperDARN radar network [http://vt.superdarn.org/tiki/assets/pages/fov/all/allfovs_20161020.png].

Analysis-*SZA*

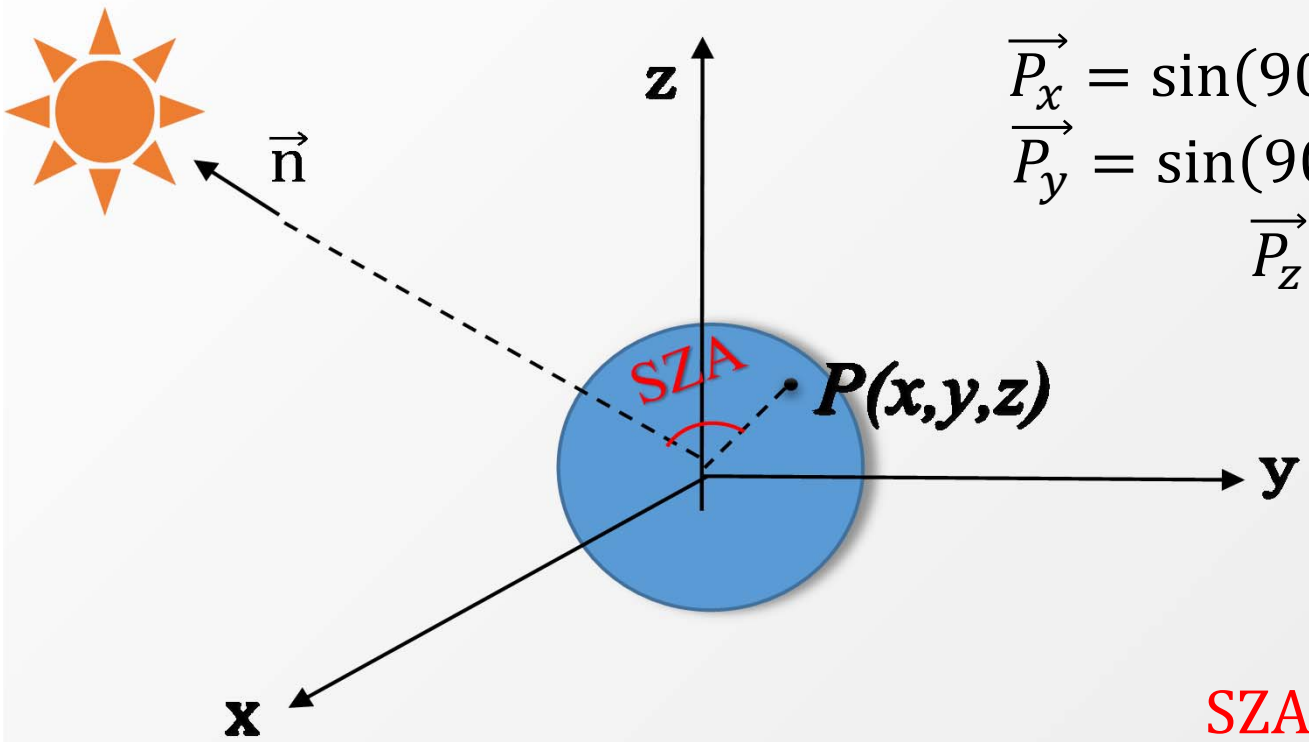

$$\overrightarrow{P_x} = \sin(90° - \text{glat}) \times \cos(\text{glon})$$
$$\overrightarrow{P_y} = \sin(90° - \text{glat}) \times \sin(\text{glon})$$
$$\overrightarrow{P_z} = \cos(\text{glon})$$

$$\text{SZA} = \arccos(\vec{\text{n}} \cdot \vec{\text{p}})$$

Discussion 1-2

- SAPS happens more often in winter than other seasons.

① The time period is set to 0300~0900 UT, if you take a longer span, there should be more SAPS events happen in other seasons.

② Other than winter, the ionosphere is illuminated entirely, so it might be more difficult to generate a strong electric field or to observe the ionospheric echoes.

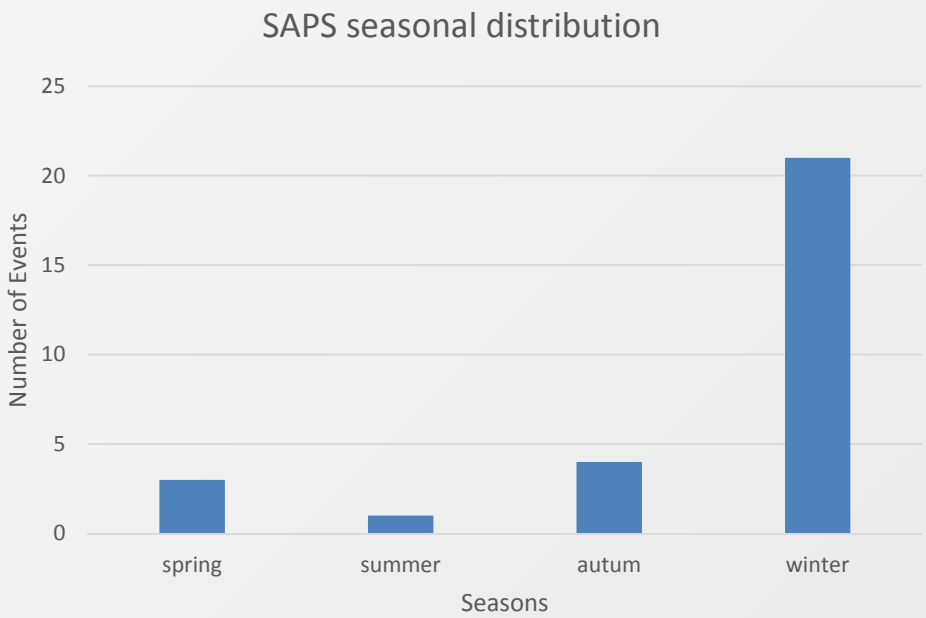

Discussion 3

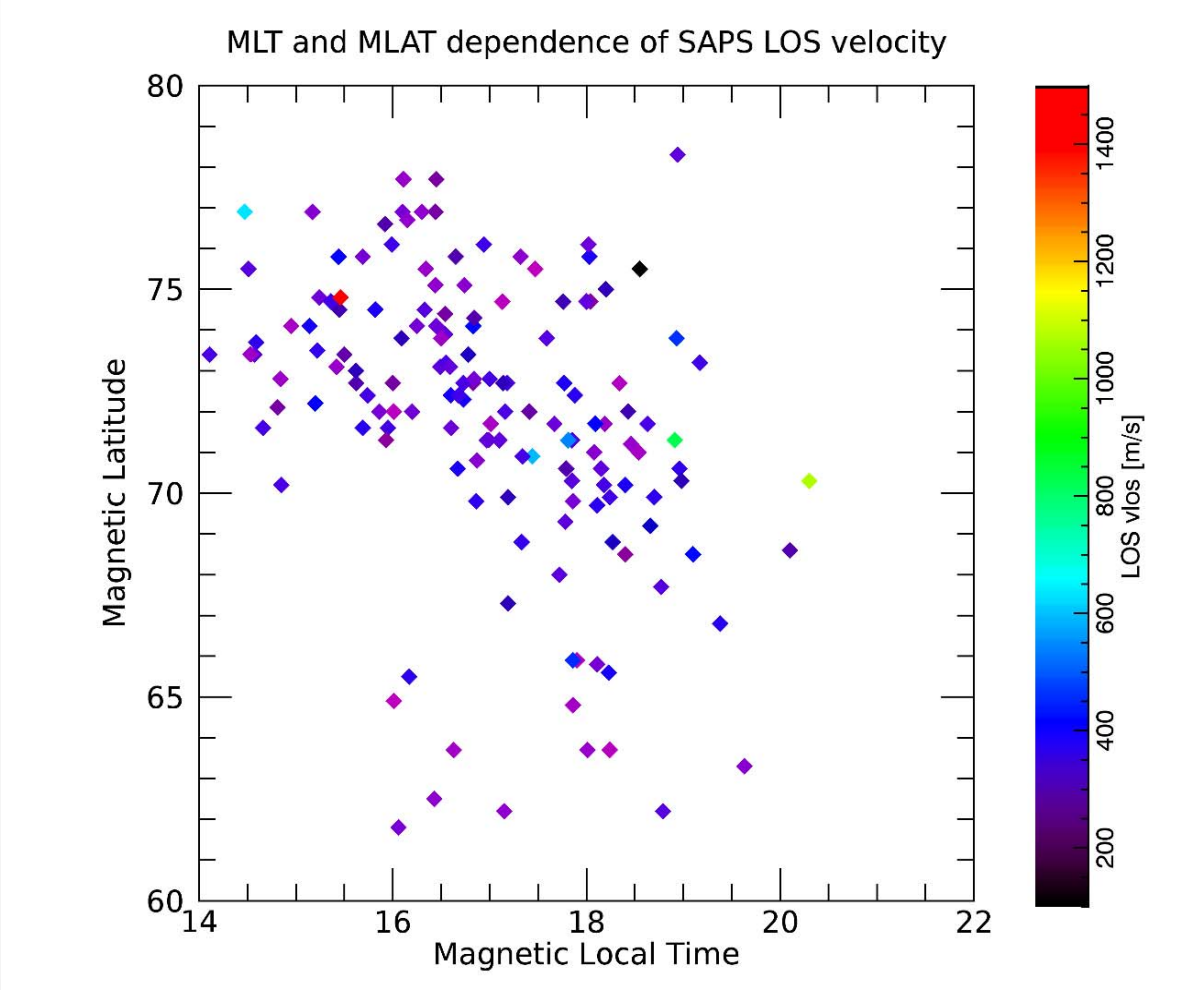

Introduction

- A solar zenith angle controlled conductivity could be expected for low Kp values and particularly for Pederson conductivities (∑p) [Schlegel, 1988].

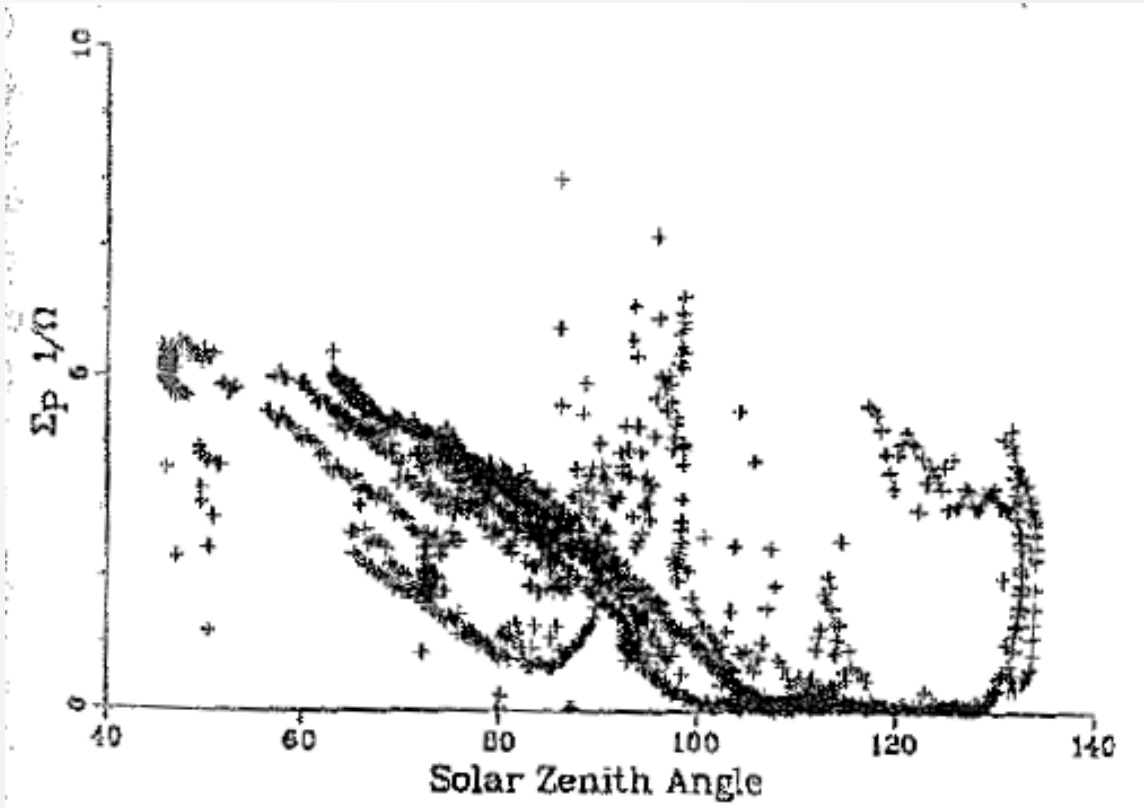

[Schlegel, 1988]

Instrumentations

- SuperDARN Hokkaido East Radar
  Location: +36.76, -144.78
  (AACGM magnetic coordinates)
  Time resolution: 1s ~ 2 min
  Space resolution: 15 km ~ 100 km
  Beam Width: 5 degrees

- SuperDARN Buckland Park Radar
  Location: -46.2, -146.1
  (AACGM magnetic coordinates)

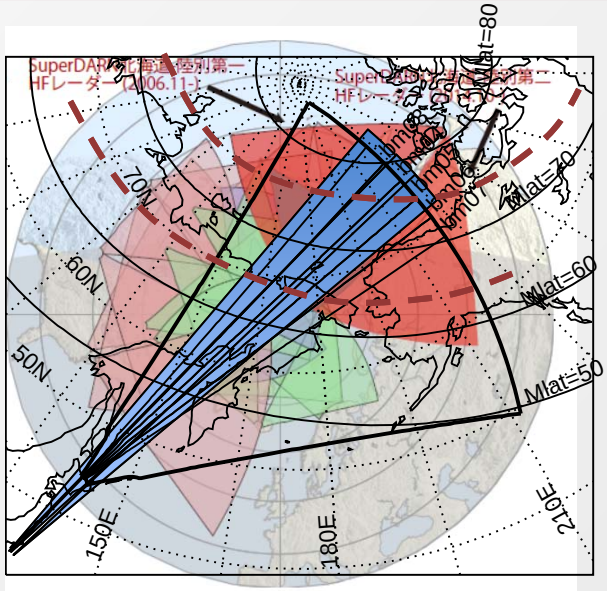

[西谷　望,2014]

- NOAA POES (Polar-orbiting Operational Environmental Satellites) Satellite System

The POES satellite system makes nearly polar orbits 14 times per day. We can exam the precipitating energy flux obtained from the total electron detector (TED) onboard the NOAA POES satellites.